NTNU
Norwegian University of
Science and Technology

Dynamic analysis of a system with RPT

Carl Andreas Veie

Master of Energy and Environmental Engineering
Submission date: June 2018
Supervisor: Torbjørn Kristian Nielsen, EPT
Co-supervisor: Magni Fjørtoft Svarstad, EPT

Norwegian University of Science and Technology
Department of Energy and Process Engineering

NTNU
Norwegian University
of Science and Technology

Department of Energy
and Process Engineering

EPT-M-2018-104

MASTER THESIS

for

Student Carl Andreas Veie

Spring 2018

Dynamic analysis of a system with RPT

Dynamisk analyse av system med RPT

Background and objective

In some hydro power plants, there are installed Reversible Pump Turbines (RPT). This are hydraulic machines that can operate in both as a turbine and as a pump. These kind of turbines are highly actualized by the demand for power operation. A PhD project is ongoing, which is focused on changing from pump mode to turbine mode of operation as fast as possible. In Spring 2018 tests of the dynamic performance at Tevla Hydro Power plant (near Meråker) will be performed.

The objective is to establish a simulation model of Tevla power plant and analyse the dynamic behaviour as the RPT goes continously from pumping to turbine mode of opertaion. The same analysis shall be done for the test rig at the Waterpower Laboratory.The model will be verified by the tests performed at the Waterpower Laboratory and at Tevle power plant.

The following tasks are to be considered:

1. Complete and improve the simulation model made during the candidates project
2. Simulate the Waterpower Laboratory and verify by the tests previously performed
3. Simulate Tevla power plant
4. Participate in the tests at Tevla and verify the simulations
5. If the student will go to Nepal for a excursion, earlier and further work will be presented as a publication and presented at the conference; 8th *International symposium on Current Research in Hydraulic Turbines (CRHT-VIII)* at Kathmandu University in March 2018

-- " --

Within 14 days of receiving the written text on the master thesis, the candidate shall submit a research plan for his project to the department.

When the thesis is evaluated, emphasis is put on processing of the results, and that they are presented in tabular and/or graphic form in a clear manner, and that they are analyzed carefully.

The thesis should be formulated as a research report with summary both in English and Norwegian, conclusion, literature references, table of contents etc. During the preparation of the text, the candidate should make an effort to produce a well-structured and easily readable report. In order to ease the evaluation of the thesis, it is important that the cross-references are correct. In the making of the report, strong emphasis should be placed on both a thorough discussion of the results and an orderly presentation.

The candidate is requested to initiate and keep close contact with his/her academic supervisor(s) throughout the working period. The candidate must follow the rules and regulations of NTNU as well as passive directions given by the Department of Energy and Process Engineering.

Risk assessment of the candidate's work shall be carried out according to the department's procedures. The risk assessment must be documented and included as part of the final report. Events related to the candidate's work adversely affecting the health, safety or security, must be documented and included as part of the final report. If the documentation on risk assessment represents a large number of pages, the full version is to be submitted electronically to the supervisor and an excerpt is included in the report.

Pursuant to "Regulations concerning the supplementary provisions to the technology study program/Master of Science" at NTNU §20, the Department reserves the permission to utilize all the results and data for teaching and research purposes as well as in future publications.

The final report is to be submitted digitally in DAIM. An executive summary of the thesis including title, student's name, supervisor's name, year, department name, and NTNU's logo and name, shall be submitted to the department as a separate pdf file. Based on an agreement with the supervisor, the final report and other material and documents may be given to the supervisor in digital format.

☐ Work to be done in lab (Water power lab, Fluids engineering lab, Thermal engineering lab)
☒ Field work

Department of Energy and Process Engineering, 15. January 2018

Torbjørn K. Nielsen
Academic Supervisor

Research Advisor: Magni Fjørtoft Svarstad

Preface

First of all I want to express my most sincere gratitude to my supervisors Torbjørn Nielsen and Magni Fjørtoft Svarstad for all guidance and discussions during the semester. I also want to thank my fellow students at the Waterpower Laboratory for a great year together, and for creating such a nice and social environment. A special thanks to Daniel Sannes for his help and to Knut Ringstad for valuable discussions. Finally, thanks to Thomas Svensson Moen, Jarl Øystein Samseth, Karoline Aker Christiansen and Albert Mugisha for proofreading.

Carl Andreas Veie
Trondheim, June 11th 2018.

Abstract

The purpose of this master's thesis is to establish and validate a simulation model of the transition from pump to turbine mode of operation for hydropower systems with reversible pump-turbines (RPTs). The model builds on the one-dimensional turbine model presented by Nielsen [1], but uses pump mode of operation as a basis. Simulations have been carried out in MATLAB, and compared with measurements from the RPT rig at the Waterpower Laboratory at NTNU.

Simulation of transition from pump mode to turbine mode was conducted by cutting the torque from the motor that drives the RPT in pump mode. This reduces the rotational speed of the runner and it starts rotating in the other direction due to the hydraulic torque from the water, and ends up at runaway speed in turbine mode.

The results from the simulations and measurements are fairly similar in pump mode, but very different in turbine mode. At the end point of the simulations the rotational speed is only 1/3 of the speed at the end point of the measurements. There are several reasons for this difference, but insufficient accuracy of the model of the pump-turbine characteristics in turbine mode plays an important role. The model does not take into account that there are two different heads for zero flow depending on whether the RPT is going from pump to pump brake or from turbine to reverse pump mode. The simulation results are also influenced by the assumption of neglecting elasticity and the switch of causality between pump and turbine mode. Torque is the controlling parameter in pump mode, while this is the role of the hydraulic head in turbine mode. All these factors are part of the explanation of why the simulations do not follow the same trajectory as measurements in the H-Q-diagram.

Sammendrag

Hensikten med denne masteroppgaven er å etablere og validere en simuleringsmodell for overgangen fra pumpe- til turbindrift for vannkraftverk med reversible pumpeturbiner (RPT). Modellen er basert på den endimensjonale turbinmodellen utviklet av Nielsen [1], men tar utgangspunkt i pumpedrift. Simuleringene har blitt utført i MATLAB, og sammenlignet med målinger fra RPT-riggen ved Vannkraftlaboratoriet på NTNU.

Simuleringer av overgangen fra pumpe- til turbindrift ble gjennomført ved å kutte dreiemomentet fra motoren som driver RPTen i pumpemodus, noe som gjør at løpehjulet bremser opp og begynner å rotere motsatt vei på grunn av det hydrauliske dreiemomentet fra vannet.

Resultatene fra simuleringene stemmer godt overens med eksperimentelle resultater i pumpemodus, men det er store avvik i turbinmodus. Turtallet ved sluttpunktet for simuleringen er kun 1/3 av det målte turtallet. Det er flere årsaker til dette avviket, men unøyaktig representasjon av turbinmodus i modellen av pumpeturbinkarakteristikken er nok den viktigste faktoren. Modellen tar ikke hensyn til at det er ulikt trykk ved null volumstrøm avhengig av om RPTen er ved overgangen fra pumpe til bremsemodus i pumpe, eller fra turbin til revers pumpedrift. Simuleringsresultatene er også påvirket av at elastisitet ikke er inkludert i modellen og at kausaliteten i systemet endrer seg fra pumpe- til turbindrift. Mekanisk dreiemoment er kontrollerende parameter i pumpedrift, mens trykket har denne rollen i turbindrift. Disse faktorene forklarer hvorfor simuleringene ikke følger samme forløp som målingene i H-Q-diagrammet.

List of Figures

2.1 The principle operation of a RPT in pump and turbine mode [10] . . 3
2.2 Head in pump and turbine mode for an RPT [11] 4
2.3 The difference between a Francis runner and an RPT runner [3] . . . 4
2.4 Inlet and outlet velocity diagrams [14] 10
2.5 Pump characteristics, modified from [11] 11
2.6 Simple sketch of the RPT rig at the Waterpower Laboratory 13

3.1 Comparison of the model of the pump characteristics and measurements by Stranna 15
3.2 Pump-turbine characteristics for various rotational speeds 16
3.3 $n_{ED} - Q_{ED}$-diagram showing the different modes of operation for an RPT [7] 17
3.4 Operating point for the RPT before load rejection, $Q_0 = 0.120m^3/s$ and H=12.26 m. The pump characteristics is drawn for $n = 480$ rpm. 18

4.1 Transition from pump to turbine mode in H-Q-diagram 21
4.2 Transition from pump to turbine mode in n_{ED}-Q_{ED}-diagram 22
4.3 Results from simulation of load rejection, t_{max}= 6 s 23
4.4 Results from simulation of load rejection, t_{max}= 100 s 24
4.5 Comparison of the head during load rejection in measurement and simulation 25
4.6 Comparison of the rotational speed during load rejection in measurement and simulation 26
4.7 Transition from pump to turbine mode in H-Q-diagram, with modified characteristics 27
4.8 Transition from pump to turbine mode in n_{ED}-Q_{ED}-diagram, with modified characteristics 28
4.9 Pump-turbine characteristics based on measurements compared to model 29

5.1 Pump and turbine characteristics [15] 32

Nomenclature

Symbol	Description	Unit
A	Area	m^2
A_s	Surface area of surge shaft	m^2
B	Width	m
c	Absolute velocity	m/s
D	Diameter	m
g	Gravitational constant	m/s^2
H	Hydraulic head (piezometric head)	m
H_{pt}	Head over the RPT	m
H_s	Head required by the system	m
H_{st}	Static head	m
I_h	Hydraulic inertia	s/m^2
I_p	Polar moment of inertia	kgm^2
k_f	Friction coefficient	$[-]$
L	Length	m
n	Rotational speed	rpm
P	Power	W
T_h	Hydraulic torque	Nm
T_m	Mechanical torque	Nm
u	Peripheral velocity	m/s
Q	Volumetric flow rate	m^3/s
V	Volume	m^3
z	Surge shaft level	m

Greek letters

Symbol	Description	Unit
β	Relative flow angle	rad
η	Efficiency	[–]
λ	Darcy-Weisbach friction factor	[–]
ρ	Density	kg/m^3
ω	Angular velocity	rad/s

Abbreviation

Symbol	Description
RPT	Reversible pump-turbine

Table of contents

Preface i

Abstract iii

Sammendrag v

List of figures vii

Nomenclature ix

1 Introduction 1
1.1 Previous work 2

2 Theory 3
2.1 Introduction to reversible pump-turbines 3
2.2 Derivation of dynamic model 6
2.2.1 Hydraulic equation 6
2.2.2 Torque equation 7
2.2.3 Surge shaft equation 9
2.3 Pump and turbine characteristics 10
2.4 Dynamic simulation model of the Waterpower Laboratory 13

3 Method 15
3.1 Model of the characteristics of the RPT at the Waterpower Laboratory 15
3.2 Setup of simulation program 18

4 Results 21
4.1 Simulation of load rejection 21
4.2 Simulations of load rejection with modified pump-turbine characteristics 27
4.3 Characteristics based on measurements 29

5 Discussion 31

6 Conclusion 35

7 Further work **37**

Bibliography **39**

Appendix **41**

1 Introduction

Renewable energy sources constitute an increasing part of the European energy mix. In 2015 renewable energy constituted 77 % of the annual new generating capacity in Europe, making it the eighth consecutive year in which the majority of new capacity came from renewable sources [2]. The increase in intermittent energy sources like wind and solar continues to change the power market in Norway as well as in Europe. There is a rising need of higher power capacity, both of the ability to supply energy when the production from these sources is low, and to store energy when it is high. Hydropower does already play an important role in this situation because of the capacity of both short term and long term storage, and the ability of supplying energy whenever needed in order to balance the consumption. Pumped hydro storage plants are especially interesting in this respect, as they are able to pump water to a higher reservoir for storage. This can be done having separate pumps and turbines installed or by using reversible pump-turbines (RPTs). The latter have the opportunity for a fast change from pump mode to turbine mode, which meets an important requirement in a increasingly complex energy market, where the task of balancing the production and consumption of energy is becoming more and more difficult.

A fast transition from pump mode to turbine mode in a pumped hydro storage plant can be done by instantly cutting the torque from the motor that is driving the RPT in pump mode. This makes the water flow back through the runner, and it starts rotating in the opposite direction in turbine mode. Here load rejection is referred to as the entire process from cutting the torque until reaching runaway speed in turbine mode when the guide vanes opening is kept constant, even though this term normally refers to the process where the guide vanes are closing so that runner does not reach runaway speed [3].

The objective of this master thesis is to establish a simulation model and use it to analyze the dynamic behaviour of an RPT system during the transition from pump to turbine mode. The simulations could provide information that can be valuable when assessing the possibility of performing this transition at real size power plants in the future. Measurements from Tevla Power Plant and the Waterpower Laboratory were supposed to be used for validation of the simulation results, but only the latter case has been analyzed due to problems with the flow measurements from Tevla Power Plant.

1.1 Previous work

Both reversible pump-turbines and dynamic analysis of hydropower plants are fields with a lot of publications during the last decades. Nielsen [1] conducted measurements of the dynamic characteristics of a Francis turbine model at NTNU in 1990. He also presented a one-dimensional model for high head Francis turbines, which has been further developed by Nielsen [4] and Walseth [5] to be applicable for RPTs as well. Walseth wrote a PhD on dynamic behaviour of reversible pump-turbines in turbine mode of operation, and introduced a correction for the pumping effect in the torque equation. Olimstad designed a model scale RPT at the Waterpower Laboratory in 2010 as a part of his PhD on characteristics of reversible pump-turbines. The main objective was to investigate stability in turbine mode, but the model became subject to several experiments in the following years. Tests in pump mode were performed by Stranna [6] in 2012, resulting in the measurement of the pump characteristics, which have been used for comparison and adjustments of the model of the pump-turbine characteristics in this thesis. The transition from pump mode to turbine mode by means of load rejection has been the topic of the PhD work of Svarstad [7], who conducted measurements at Tevla Power Plant and at the RPT rig at the Waterpower Laboratory. The latter have been used for validation of the simulation model presented in this thesis.

This work is a continuation of a project thesis [8] written in 2017, where a simulation model of RPTs in pump mode of operation was established. The simulation model is further developed in this master's thesis to be used in turbine mode as well. The main difference compared with previous work is that pump mode is the basis for the model in this thesis, instead of turbine mode.

2 | Theory

This section presents relevant theory for performing dynamic analysis of RPTs during load rejection, including the derivation of the differential equations used in the simulation model and the model of the pump-turbine characteristics.

2.1 Introduction to reversible pump-turbines

A reversible pump-turbine (RPT) is a combination of a centrifugal pump and a Francis turbine, and is designed to operate both as a pump and as a turbine. Pumps transfer energy to a liquid by means of a rotating impeller, lifting the water from a lower to a higher reservoir. Francis turbines, on the other hand, convert the hydraulic energy from water flowing from a higher to a lower reservoir into mechanical energy in the shaft, which is used to drive a generator. This difference is illustrated in Figure 2.1 The pump head H_{np} is higher than the turbine H_{nt} because the the pump has to overcome the friction losses h_f in the waterway as well as the static head H_{st}, while the turbine head is $H_{st} - h_f$, as shown in Figure 2.2. Because H_{np} is decisive in the design of the runner of an RPT, the runner geometry is more similar to a centrifugal pump than a Francis turbine. The most obvious geometrical difference between RPTs and Francis turbines is that RPTs have longer blades that are tilted backwards in order to be able to pump and to have stability in pump mode [9], as seen in Figure 2.3.

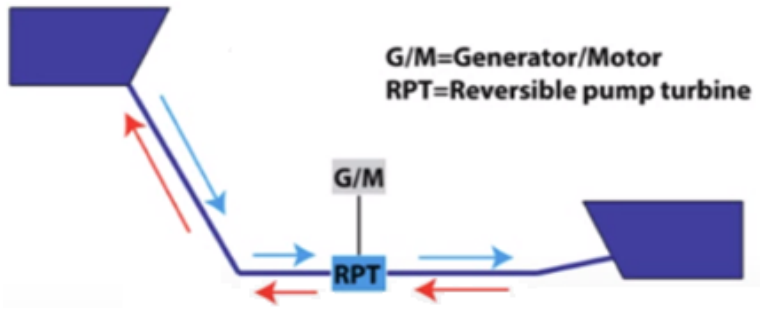

Figure 2.1: The principle operation of a RPT in pump and turbine mode [10]

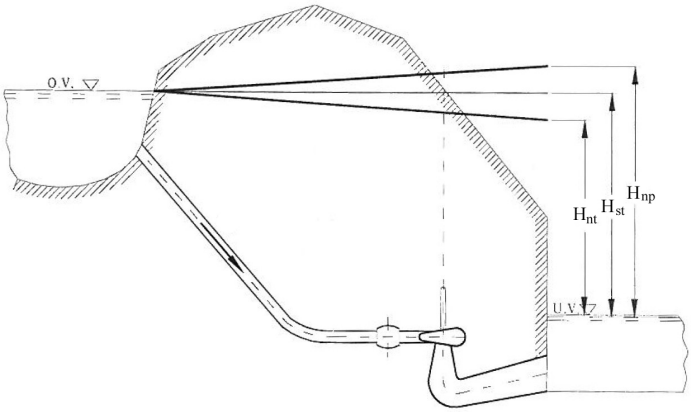

Figure 2.2: Head in pump and turbine mode for an RPT [11]

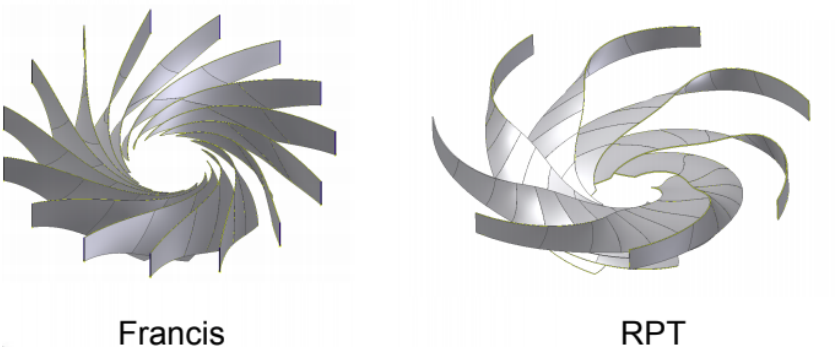

Figure 2.3: The difference between a Francis runner and an RPT runner [3]

When operating in pump mode, the generator is working as a motor, transferring energy to the RPT. In turbine mode, the runner is rotating in the opposite direction, and energy is being transferred from the runner to the generator by the shaft. The RPT can go directly from pump mode to turbine mode when the torque from the motor is removed, either due to fault or by intention. Fast transition from pump mode to turbine mode by cutting the torque while keeping the guide vane opening constant will here be referred to as load rejection. When this happens, the water will slow down, and start flowing back through the runner, forcing it to rotate in the opposite direction in turbine mode. The rotational speed of the runner increases until it reaches runaway speed. At this point the centrifugal pumping effect from the runner on the water is equal to the hydraulic energy extracted from the water, and the hydraulic efficiency is zero. By choosing a guide vane opening that gives a runaway speed that corresponds to a synchronous speed, the RPT can be connected

to the generator and deliver power to the grid. The possibility of a fast transition from pump mode to turbine mode makes the RPT able to go from storing energy to producing energy in a short period of time, which introduces more flexibility into the power system.

In pump mode, the operating points of an RPT are usually represented in a head-capacity diagram, or H-Q-diagram. The curve is referred to as the pump characteristics. In turbine mode, it is more common to present the results using the dimensionless flow and rotational speed, Q_{ED} and n_{ED}. These are defined according to Equation 2.1 and 2.2.

$$Q_{ED} = \frac{Q}{D^2\sqrt{gH}} \tag{2.1}$$

$$n_{ED} = \frac{nD}{\sqrt{gH}} \tag{2.2}$$

D refers to the outlet diameter in turbine mode.

2.2 Derivation of dynamic model

The dynamic simulation model consists of a set of ordinary differential equations, and is here applied for simulation of the transient behaviour of an RPT system during load rejection. It is based on the one-dimensional turbine model presented by Nielsen [1], and consists of a hydraulic equation and a torque equation. In addition to this, a continuity equation at the node near the surge shaft is included in the model.

2.2.1 Hydraulic equation

The hydraulic equation can be derived from the equation of motion (Equation 2.3).

$$g\frac{\partial H}{\partial x} + \frac{\partial V}{\partial t} + \frac{g}{L}h_f = 0 \tag{2.3}$$

H is the hydraulic head, which is the sum of the hydraulic pressure and the geostatic head $[m]$, V is the velocity of the flow $[m/s^2]$, L is the conduit length [m] and h_f is the head loss due to friction $[m]$.

Inserting $Q = VA$ and $\frac{\partial H}{\partial x} = \frac{H_2 - H_1}{L}$ gives:

$$\frac{L}{gA}\frac{\mathrm{d}Q}{\mathrm{d}t} = H_1 - H_2 - h_f \tag{2.4}$$

By introducing the hydraulic inertia $I_h = \frac{L}{A}$ it can be rewritten as

$$I_h\frac{\mathrm{d}Q}{\mathrm{d}t} = g(H_1 - H_2 - h_f) \tag{2.5}$$

The friction loss is approximated using the Darcy-Weisbach equation [12]:

$$h_f = \lambda\frac{L}{D}\frac{Q|Q|}{2gA^2} \tag{2.6}$$

λ is the friction factor of the conduit and D is the diameter $[m]$. From Equation 2.6 it can be seen that the friction loss can be written as $\Delta h = k_f Q|Q|$, where $k_f = \frac{\lambda L}{2gDA^2}$. The use of absolute value notation makes sure the head loss is always working against the direction of the flow.

For a simple RPT system without surge shaft the hydraulic equation (Equation 2.5) can be rewritten as

$$\frac{\mathrm{d}Q}{\mathrm{d}t} = \frac{g}{I_h}(H_{pt} - H_{st} - k_f Q|Q|) \tag{2.7}$$

Here H_{pt} is the head over the RPT, modelled according to Equation 2.31, which derived in Section 2.3. During stationary operation the flow rate Q is constant, which gives the following solution:

$$H_{pt} = H_{st} + k_f Q|Q| \tag{2.8}$$

This means that during stationary operation in pump mode, the head from the RPT must overcome the static head difference as well as the friction losses in order to deliver flow to the upper reservoir.

2.2.2 Torque equation

The torque equation can be derived from the balance of power over the turbine and generator (Equation 2.9) [13].

$$P_m = I_p \omega \frac{\mathrm{d}\omega}{\mathrm{d}t} + P_h \tag{2.9}$$

Here P_m is the electrical power from the generator working as a motor [W], I_p is polar moment of inertia of the rotating masses $[kgm^2]$, ω is the angular velocity of the runner [rad/s] and P_h is the hydraulic power transferred from the pump-turbine to the water [W].

Inserting $P_m = T_m \omega$ and dividing by ω gives:

$$\frac{\mathrm{d}\omega}{\mathrm{d}t} = \frac{1}{I_p}(T_m - T_h) \tag{2.10}$$

T_h is the hydraulic torque from the water to the shaft in turbine mode, and the torque from the shaft acting on the water in pump mode. T_m is the mechanical torque from from the shaft to the generator in turbine mode, and torque from the generator to the shaft in pump mode. The generator and the runner are rotating masses that are accelerated when there is a difference between the hydraulic torque and the mechanical torque from the generator. Under regular operating conditions in pump mode and turbine mode, the hydraulic torque is given by the following equation:

$$T_h = \frac{\rho g Q H_p}{\omega \eta_p} \tag{2.11}$$

However, due to the singularity as ω approaches zero, this equation cannot be used to simulate load rejection [8]. An alternative version of the hydraulic torque equation is applied instead. It was presented by Nielsen [1, 4] and further developed by Walseth [5]. The derivation presented here is based on the previous work on this equation, with some modifications.

The torque transferred from the runner to the water in pump mode can be expressed as [14]:

$$T_h = \rho Q(r_2 c_{u2} - r_1 c_{u1}) \tag{2.12}$$

Using the velocity diagrams in Figure 2.4, the equation can be rewritten:

$$T_h = \rho Q(r_2 c_2 \cos\alpha_2 + r_1 A_z \cot\beta_1 c_2 \sin\alpha_2 - r_1^2\omega) \tag{2.13}$$

Here A_z is the ratio of the outlet area to the inlet area of the runner. The torque when the impeller is at rest is given by the first two terms, called the specific starting torque $t_s = r_2 c_2 \cos\alpha_2 + r_1 A_z \cot\beta_1 c_2 \sin\alpha_2$. Hence the torque can be rewritten according to Equation 2.14.

$$T_h = \rho Q(t_s - r_1^2\omega) \tag{2.14}$$

The hydraulic efficiency in pump mode is given by Equation 2.15.

$$\eta_h = \frac{\rho g Q H}{T_h \omega} = \frac{gH}{(t_s - r_1^2\omega)\omega} \tag{2.15}$$

When the guide vane angle is optimal (α_2=α_2^*), the efficiency is maximal and $\frac{\partial \eta_h}{\partial \alpha_2} = 0$.

$$\frac{\partial \eta_h}{\partial \alpha_2} = \frac{gH}{\omega} \frac{-r_2 c_2 \sin\alpha_2^* + r_1 A_z \cot\beta_1 c_2 \cos\alpha_2^*}{(r_2 c_2 \cos\alpha_2 + r_1 A_z \cot\beta_1 c_2 \sin\alpha_2 - r_1^2\omega)^2} = 0 \tag{2.16}$$

This gives $\cot\beta_1 = \frac{r_2}{A_z r_1} \tan{\alpha_2}^*$, which is substituted into t_s to obtain Equation 2.17.

$$t_s = r_2 c_2(\cos\alpha_2 + \tan\alpha_2^* \sin\alpha_2) \tag{2.17}$$

Inserting this result into Equation 2.14, and using $c_2 = \frac{c_{m2}}{\sin\alpha_2} = \frac{Q}{A_2 \sin\alpha_2}$ to obtain:

$$T_h = \rho|Q| \left(r_2 \frac{Q}{A_2}(\cot\alpha_2 + \tan\alpha_2^*) - r_1^2\omega \right) \tag{2.18}$$

The absolute value sign is included in order to make sure that the torque is always positive, so that the hydraulic torque contributes to increase the rotational speed in turbine mode until it reaches a stable point of operation.

In order to account for differences between a regular Francis turbine and a reversible pump-turbine, the equation was modified by including a pumping effect [5], given by the last two terms in Equation 2.19.

$$T_h = \rho|Q| \left(r_2 \frac{Q}{A_2}(\cot\alpha_2 + \tan\alpha_2^*) - r_1^2\omega + \Gamma\omega - R_p Q \right) \tag{2.19}$$

Here $\Gamma = (r_2^2 - r_1^2)$ and $R_p = \frac{r_2}{A_2 \tan\beta_2} - \frac{r_1}{A_1 \tan\beta_1}$. Inserting this result into Equation 2.10 gives:

$$\frac{\mathrm{d}\omega}{\mathrm{d}t} = \frac{1}{I_p} \left(T_m - \rho|Q|(r_2 \frac{Q}{A_2}(\cot\alpha_2 + \tan\alpha_2^*) - r_1^2\omega + \Gamma\omega - R_p Q) \right) \tag{2.20}$$

This model does not account for the losses in the energy transfer, as it assumes that all mechanical energy is transferred into hydraulic energy.

2.2.3 Surge shaft equation

In the simulation model of the Waterpower Laboratory, the pressure chamber is substituted with a surge shaft with an equivalent area $A_s = 3.8\ m^2$ that should give the same effect as the chamber, according to Equation 2.21 [13].

$$A_s = \frac{1}{\frac{1}{A_{pc}} + \frac{\kappa h_{p0}}{V_0}} \tag{2.21}$$

Here A_s is the surge shaft area $[m^2]$, h_{p0} is the initial absolute pressure in the chamber [Pa], v_0 is the initial volume of air $[Nm^3]$, A_{pc} is the surface area covered with water in the pressure chamber $[m^2]$, κ is the ratio of specific heat, also known as the adiabatic exponent, which is equal to 1.4 for air.

The simulation model presented in this thesis assumes inelastic conduits, and the flow is assumed constant in the axial direction in all conduits. When introducing a surge shaft to the system, the continuity equation at the node yields:

$$\frac{\mathrm{d}z}{\mathrm{d}t} = \frac{1}{A_s}(Q_1 - Q_2) \tag{2.22}$$

Here z is the level in the surge shaft, Q_1 is the flow in the lower conduit and Q_2 is the flow upper conduit. The direction of flow is defined as the direction in pump mode, which is from the lower to the upper reservoir.

2.3 Pump and turbine characteristics

The hydraulic equation (Equation 2.7) in the simulation model includes a reversible pump-turbine characteristics that covers the entire operating range. It is based on the model of pump characteristics derived in this section, and then generalized to turbine mode.

The pump characteristics can be be derived from the Euler pump equation (Equation 2.23) by subtracting different losses from the ideal pump curve, $H_{t\infty}$, as seen in from Figure 2.5. The equation shows that the energy transferred to the flow is equal to the change of the velocity vectors in direction and magnitude.

$$P = T\omega = \rho Q(u_2 c_{u2\infty} - u_1 c_{u1\infty}) \tag{2.23}$$

The inlet and outlet velocity triangles of a pump are shown in Figure 2.4. Subscript 1 is used for pump inlet and 2 for pump outlet. c_u is the component of the absolute velocity c in the direction of the peripheral velocity u.

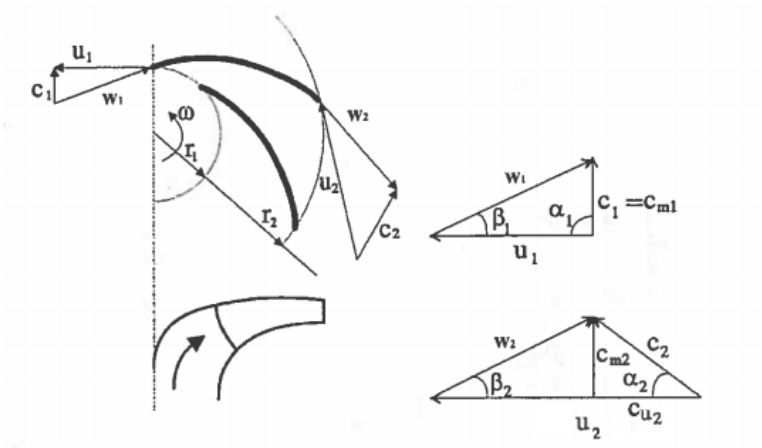

Figure 2.4: Inlet and outlet velocity diagrams [14]

An other expression for the power is

$$P = \rho g Q H_{t\infty} \tag{2.24}$$

Using Equation 2.23 and 2.24 to obtain:

$$H_{t\infty} = \frac{u_2 c_{u2\infty} - u_1 c_{u1\infty}}{g} \tag{2.25}$$

$H_{t\infty}$ is the ideal head when all losses are neglected, and assumes an infinite number of blades.

Equation 2.25 can be rewritten using the outlet velocity triangle in Figure 2.4.

$$c_{u2\infty} = u_2 - \frac{c_{m2}}{\tan\beta_{2\infty}} = u_2 - \frac{Q}{A_2 \tan\beta_{2\infty}} \tag{2.26}$$

The same can be done for c_{u1}, meaning Equation 2.25 can be rewritten:

$$H_{t\infty} = \frac{u_2}{g}\left(u_2 - \frac{Q}{A_2 \tan\beta_{2\infty}}\right) - \frac{u_1}{g}\left(u_1 - \frac{Q}{A_1 \tan\beta_{1\infty}}\right) \tag{2.27}$$

The peripheral velocity is dependent on the rotational speed of the impeller. Employing $u = \omega\frac{D}{2}$, inserting $A_2 = \pi D_2 B_2$ and $A_1 = \frac{\pi D_1^2}{4}$ gives Equation 2.28.

$$H_{t\infty} = \frac{(D_2^2 - D_1^2)}{4g}\omega^2 - \frac{Q\omega}{2\pi g}\left(\frac{1}{B_2 \tan\beta_{2\infty}} - \frac{4}{D_1 \tan\beta_{1\infty}}\right) \tag{2.28}$$

There are three main sources of losses that take place inside the pump, slip losses, friction losses and impulse losses. Slip losses occur because the pressure is higher at the side of the blade where the water hits, called pressure side, than the other side, called suction side. This pressure difference results in a force from the pressure side towards the suction side, which makes the outlet flow angle β_2 different from the blade angle $\beta_{2\infty}$. The difference, $\Delta\beta_2$, is called the slip angle.

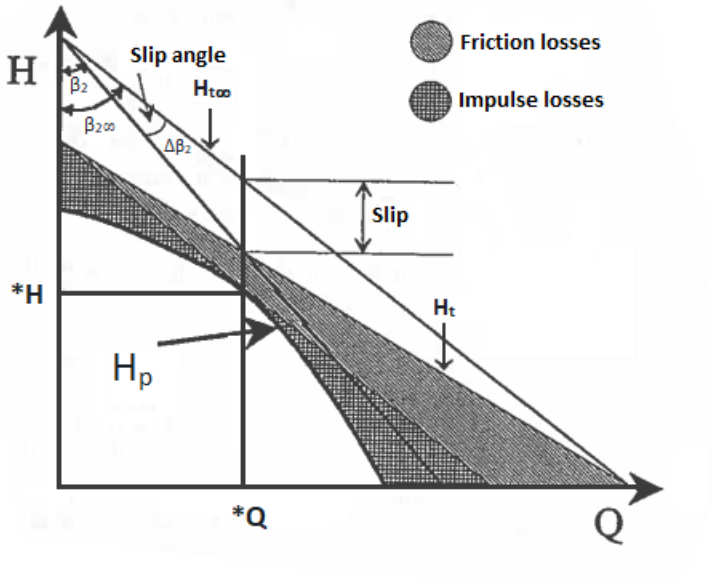

Figure 2.5: Pump characteristics, modified from [11]

When slip is taken into consideration, the head drops from $H_{t\infty}$ to H_t. The characteristics H_p is found by subtracting the hydraulic losses from the H_t-line. Hydraulic losses consist of friction losses and impulse losses. There are other kinds of losses that also are present, like leakage losses, mechanical losses and disk friction losses, but they do not directly affect the pump characteristics. Friction losses are due to skin friction between the flow and solid surfaces, and are hard to quantify for a complex geometry like a pump or a turbine. They are usually written as $k_1 Q^2$, where k_1 is a constant that includes all unknown geometrical parameters. Impulse losses, also called shock losses, take place when the direction of the flow deviates from the angle of the blade. They are written as $k_2(Q - {}^*Q)^2$, where ${}^*Q$ is the flow when the runner angle corresponds with the relative velocity of the flow so that the incident angle is zero. Quantifying the hydraulic losses is important for obtaining an accurate model of the pump characteristics, but due to the complicated geometry and flow patterns of pumps and RPTs, it is hard to predict the value of the loss coefficients k_1 and k_2 without using measurement data.

When including the losses, the following equation for the pump characteristics is obtained:

$$H_p = \frac{(D_2^2 - D_1^2)}{4g}\omega^2 - \frac{Q\omega}{2\pi g}\left(\frac{1}{B_2 \tan\beta_{2\infty}} - \frac{4}{D_1 \tan\beta_{1\infty}}\right) - k_1 Q^2 - k_2(Q - {}^*Q)^2 \tag{2.29}$$

This equation can be simplified by defining some constants:

$$H_p = H_0 \frac{\omega^2}{\omega_0^2} - a\frac{\omega}{\omega_0}Q - k_1 Q^2 - k_2(Q - {}^*Q)^2 \tag{2.30}$$

Here $H_0 = \frac{\omega_0^2}{4g}(D_2^2 - D_1^2)$ and $a = \frac{\omega_0}{2\pi g}(\frac{1}{B_2 \tan(\beta_{2\infty})} - \frac{4}{D_1 \tan(\beta_{1\infty})})$. ω_0 is a reference angular velocity, here chosen to be 58.64 rad/s (560 rpm).

The equation is based on pump mode, but can be used for modelling turbine mode as well by doing some minor modifications. The loss terms are modified in order to give more correct results when the flow turns, meaning that the full pump-turbine characteristics yields:

$$H_{pt} = H_0 \frac{\omega^2}{\omega_0^2} - a\frac{\omega}{\omega_0}Q - k_1 Q|Q| - k_2({}^*Q - |Q|)({}^*Q - Q) \tag{2.31}$$

The loss coefficients k_1 and k_2 are estimated by comparing with laboratory measurements. k_1 is estimated from the highest efficiency point on the pump characteristics, where the impulse losses are assumed to be zero, and k_2 is approximated from the head for zero flow.

2.4 Dynamic simulation model of the Waterpower Laboratory

The RPT system at the Waterpower Laboratory, sketched in Figure 2.6, is simulated using an inelastic model comprised of Equation 2.32 to 2.35. Equation 2.32 and 2.33 correspond to Equation 2.7, while Equation 2.35 corresponds to 2.20. There are two hydraulic equations because of the node at the surge shaft. Q_1 is the flow in the lower conduit, prior to the surge shaft, while Q_2 is the flow in the upper conduit. The sign convention in pump mode is applied, meaning that flow and rotational speed are defined to be positive in pump mode, and negative in turbine mode.

$$\frac{\mathrm{d}Q_1}{\mathrm{d}t} = \frac{g}{I_{h1}} \left(H_{pt} - z - k_{f1} Q_1 |Q_1| \right) \tag{2.32}$$

$$\frac{\mathrm{d}Q_2}{\mathrm{d}t} = \frac{g}{I_{h2}} \left(z - H_{st} - k_{f2} Q_2 |Q_2| \right) \tag{2.33}$$

$$\frac{\mathrm{d}z}{\mathrm{d}t} = \frac{1}{A_s} (Q_1 - Q_2) \tag{2.34}$$

$$\frac{\mathrm{d}\omega}{\mathrm{d}t} = \frac{1}{I_p} (T_m - T_h) \tag{2.35}$$

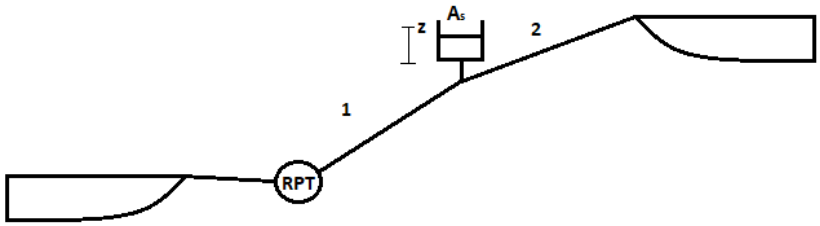

Figure 2.6: Simple sketch of the RPT rig at the Waterpower Laboratory

Table 2.1: Friction factors for the conduits in the waterway of the RPT rig at the Waterpower Laboratory

No	L $[m]$	A $[m^2]$	Re	$\frac{\epsilon}{D}$	λ	k_f
1	1.10	$1.96 \cdot 10^{-1}$	$2.87 \cdot 10^{8}$	$5.00 \cdot 10^{-2}$	$7.16 \cdot 10^{-2}$	$4.08 \cdot 10^{-2}$
2	2.69	$2.83 \cdot 10^{-1}$	$2.39 \cdot 10^{8}$	$4.17 \cdot 10^{-2}$	$6.59 \cdot 10^{-2}$	$5.31 \cdot 10^{-2}$
3	2.08	$1.26 \cdot 10^{-1}$	$3.59 \cdot 10^{8}$	$6.25 \cdot 10^{-2}$	$7.96 \cdot 10^{-2}$	$1.67 \cdot 10^{-1}$
4	8.06	$2.83 \cdot 10^{-1}$	$2.39 \cdot 10^{8}$	$4.17 \cdot 10^{-2}$	$6.59 \cdot 10^{-2}$	$1.59 \cdot 10^{-1}$
5	15.0	$9.6 \cdot 10^{-2}$	$4.10 \cdot 10^{8}$	$7.14 \cdot 10^{-2}$	$8.51 \cdot 10^{-2}$	1.93
6	4.50	$2.44 \cdot 10^{-1}$	$2.58 \cdot 10^{8}$	$4.48 \cdot 10^{-2}$	$6.81 \cdot 10^{-2}$	$1.14 \cdot 10^{-1}$

The waterway consists of 6 conduits, where number 5-6 constitute section 1 from Figure 2.6 and 1-4 make up section 2. The friction loss factors for pipe section i, k_{fi}, is calculated as $\frac{\lambda_i L_i}{2gD_i A_i^2}$. λ is calculated using Moody charts with roughness $\epsilon = 0.025$ and Reynolds number $Re_i = \frac{\rho V_i D_i}{\mu}$, where $V_i = \frac{Q_0}{A_i}$. Details are presented in Table 2.1. The hydraulic inertia I_h of the two sections was calculated by adding the L/A-ratios of the conduits.

The polar moment of inertia of the turbine and generator, I_p, is approximated using Equation 2.36.

$$I_p = \frac{T_a P}{\omega^2} \tag{2.36}$$

T_a is the time constant of the rotating masses, which is measured to 1.63 s by Svarstad, and P is the power at the measured point of operation. The available head is 12 m, Q=0.176 m^3/s, and n=416.18 rpm, which gives a polar moment of inertia of 17.76 kg^2m^2. Here the efficiency η is assumed to be 1.

3 Method

3.1 Model of the characteristics of the RPT at the Waterpower Laboratory

The characteristics in pump mode was modelled according to Equation 2.30, and a comparison between the model and stationary measurements performed by Stranna [6] are shown in Figure 3.1. There is a significant deviation between the model and the measurements for large flow, but for most part of the operating range the model approximates the measured characteristics quite accurately. Because the deviation between model and measurements is smaller when neglecting slip losses, they have not been included in Equation 2.30.

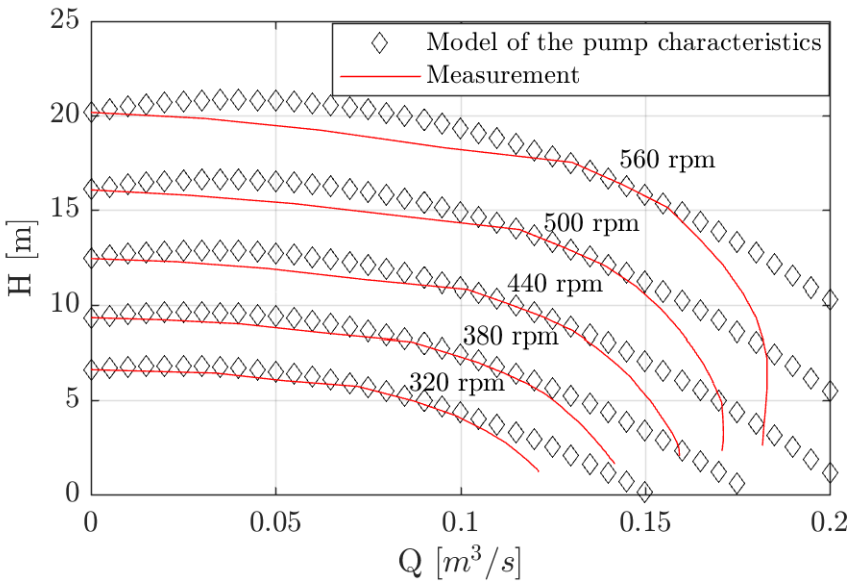

Figure 3.1: Comparison of the model of the pump characteristics and measurements by Stranna

The characteristics for different rotational speeds are drawn in Figure 3.2. Operation in pump mode is defined as positive direction for both rotational speed and flow rate. The first quadrant is regular pump mode, while both pump brake mode and turbine mode are found in the second quadrant. In pump brake mode the rotational speed is positive, while in turbine mode it is negative. According to the model, the head in turbine mode is slightly lower than in pump brake mode, and the difference is proportional to the flow. During load rejection, the operating point of the RPT moves from pump mode in the first quadrant to the second quadrant, where it goes through pump brake mode before it ends up at runaway speed in turbine mode.

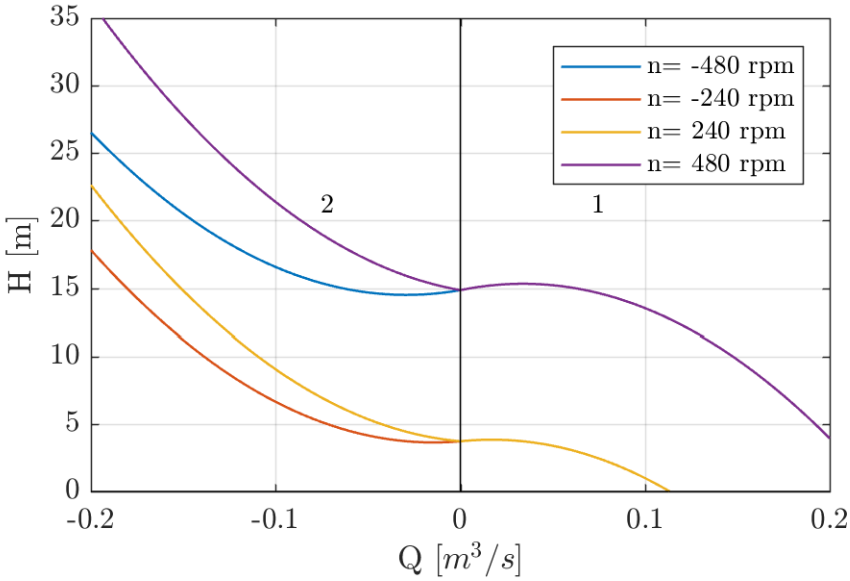

Figure 3.2: Pump-turbine characteristics for various rotational speeds

It is often more convenient to present the dynamic behaviour of pump-turbines in a $n_{ED} - Q_{ED}$-diagram (Figure 3.3) than a H-Q-diagram. This diagram is seen from the turbine side, meaning turbine mode is defined as positive direction of flow and rotational speed. There are, in general, four different modes of operation corresponding to the four different quadrants in the $n_{ED} - Q_{ED}$-diagram. These are pump mode (1), pump brake mode (2), turbine mode (3) and reverse pump mode (4). During load rejection, the RPT goes from pump mode (1), through pump break mode (2) and ends up in turbine mode (3). It does not enter into reverse pump mode (4).

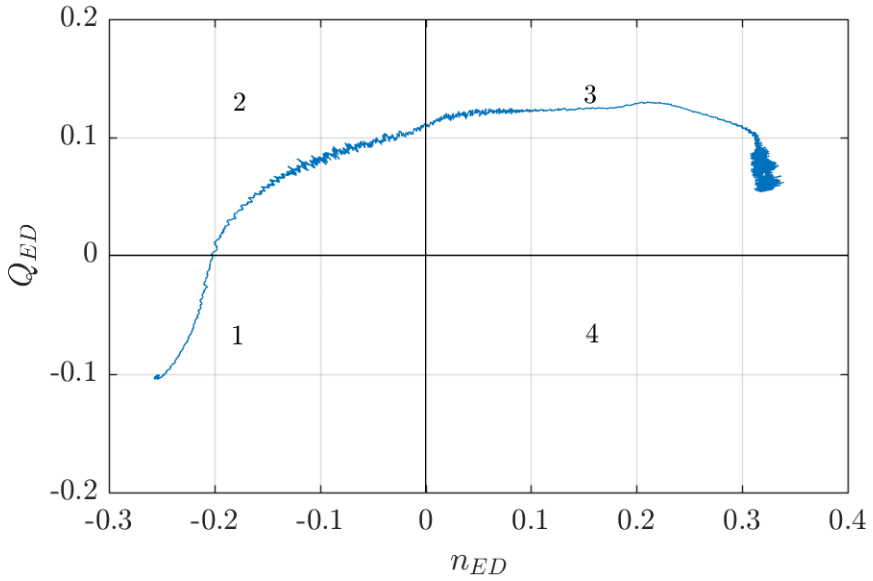

Figure 3.3: $n_{ED} - Q_{ED}$-diagram showing the different modes of operation for an RPT [7]

Stationary pump-turbine characteristics in a H-Q-diagram can also be obtained from measurements by choosing one specific speed n and converting the points in the $n_{ED} - Q_{ED}$-diagram to H-Q, using the definitions of n_{ED} and Q_{ED}.

$$H = \frac{n^2 D^2}{g n_{ED}^2} \tag{3.1}$$

$$Q = Q_{ED} D^2 \sqrt{gH} \tag{3.2}$$

This conversion gives the same characteristics for positive and negative rotational speeds. In order to tell the difference between these two cases, $\sqrt{gH} = \frac{nD}{n_{ED}}$ can be substituted into Equation 3.2 to obtain:

$$Q = \frac{Q_{ED} D^3 n}{n_{ED}} \tag{3.3}$$

3.2 Setup of simulation program

The simulations are carried out using MATLAB. Before simulating load rejection, the program calculates the initial operating point of the RPT in pump mode prior to the transition. Both the static head, H_{st}, and the initial rotational speed, ω_0, are given as input to the simulation program, while the initial flow, Q_0, and surge shaft level, z_0, are being calculated. Q_0 and z_0 are found by setting the time derivatives in the differential equations equal to zero. Q_0 is found by iteration for convergence between the pump characteristics and system characteristics, when the difference between them is smaller than an error tolerance of 10^{-3} m, as seen in Figure 3.4. The system characteristics is the sum of the static head and the friction losses. Combining Equation 2.32 and 2.33 for stationary operation gives:

$$H_{pt0} = H_{st} + (k_{f1} + k_{f2})Q_0|Q_0| \tag{3.4}$$

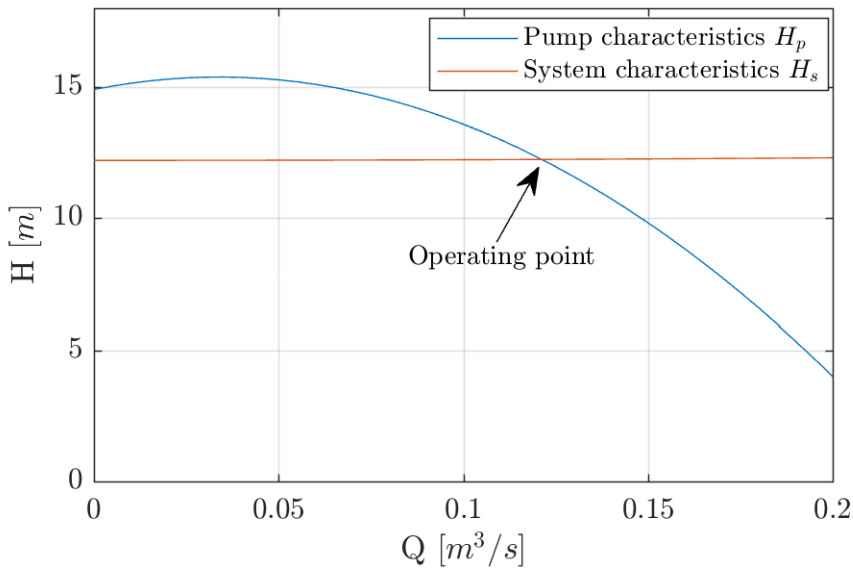

Figure 3.4: Operating point for the RPT before load rejection, $Q_0 = 0.120 m^3/s$ and H=12.26 m. The pump characteristics is drawn for $n = 480$ rpm.

As seen from the figure, the system characteristics is almost flat because of the low friction factors.

The initial head, H_{pt0}, is found from the pump-turbine model in Equation 2.31 by inserting Q_0 and ω_0, and is used to calculate the initial surge shaft level from the stationary version of Equation 2.32:

$$z = H_{pt0} - k_{f1} Q_0 |Q_0| \tag{3.5}$$

In stationary operation the hydraulic torque and the motor torque are equal, thus the initial mechanical torque is given by:

$$T_{m0} = T_{h0} = \rho |Q_0| \left(r_2 \frac{Q_0}{A_2} (\cot \alpha_2 + \tan \alpha_2^*) - r_1^2 \omega_0 \right) \tag{3.6}$$

The initial conditions of the variables in the model are chosen to be as close as possible to measurement values. The initial rotational speed is set to 480.95 rpm, and the static head is set to 12.26 m.

The equations are solved numerically using ode45, an integrated function for solving ODEs in MATLAB. ode45 integrates the system of differential equations for the specified set of initial conditions for flow rate, surge shaft level and rotational speed over a given time span. Load rejection is simulated by setting the mechanical torque T_m equal to zero at the initial time step, and then simulating until the RPT has reached runaway speed in turbine mode.

4 Results

4.1 Simulation of load rejection

The simulations of load rejection for the RPT at the Waterpower Laboratory are shown in Figure 4.1 and 4.2, along with measurements by Svarstad for comparison [7]. Simulations are carried out with an initial rotational speed of 480.95 rpm and a static head of 12.26 m. The transition between pump brake and turbine mode in the measurements, i.e. when the rotational speed is zero, is marked with a green dot.

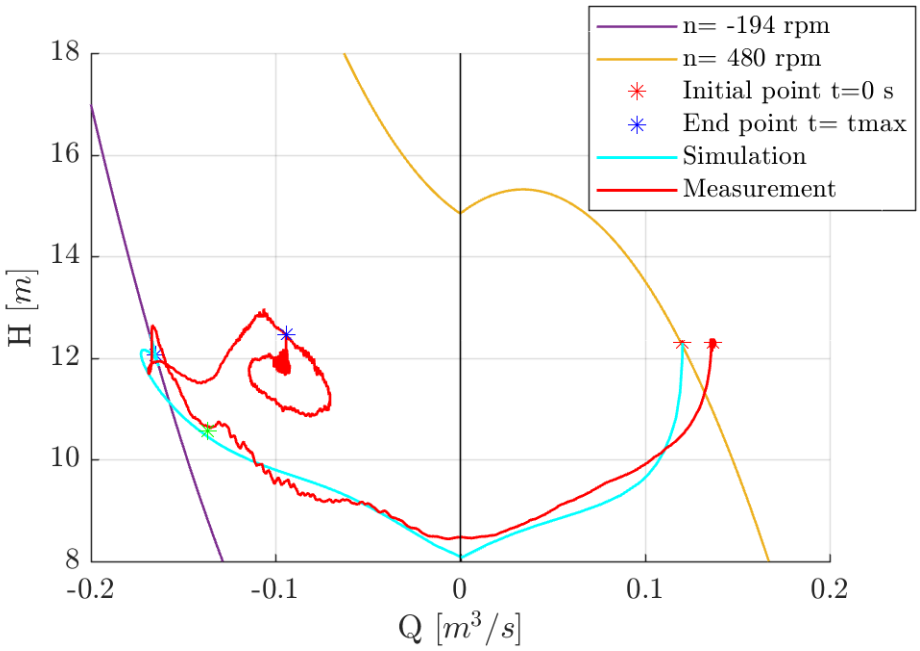

Figure 4.1: Transition from pump to turbine mode in H-Q-diagram

Figure 4.1 shows the dynamic trace of the operating point of the RPT during load rejection for both simulation and measurement. Stationary characteristics are drawn for the rotational speed at the initial point and the end point of the simulation, making it easier to see how the RPT goes from n=480 rpm at the initial point to n=-194 rpm.

Measured and simulated transitions match quite well in pump and pump brake mode, but differ in turbine mode. The measurements give a runaway speed of -597 rpm, while the simulation gives only -194 rpm. As seen in the figure, the trajectory of the measurement continues past the end point of the simulation, and turns several times before it stops.

The initial operating point in the model is different from the measurements. A deviation between the measurements by Stranna and Svarstad is the main reason for this, as the former was used as a basis for the pump characteristics, while the latter is used for comparison in the figure. This is probably related to differences in the way these measurements were conducted, as Stranna used a closed loop while Svarstad used an open loop set up. Simulations that account for this deviation are presented in Section 4.2.

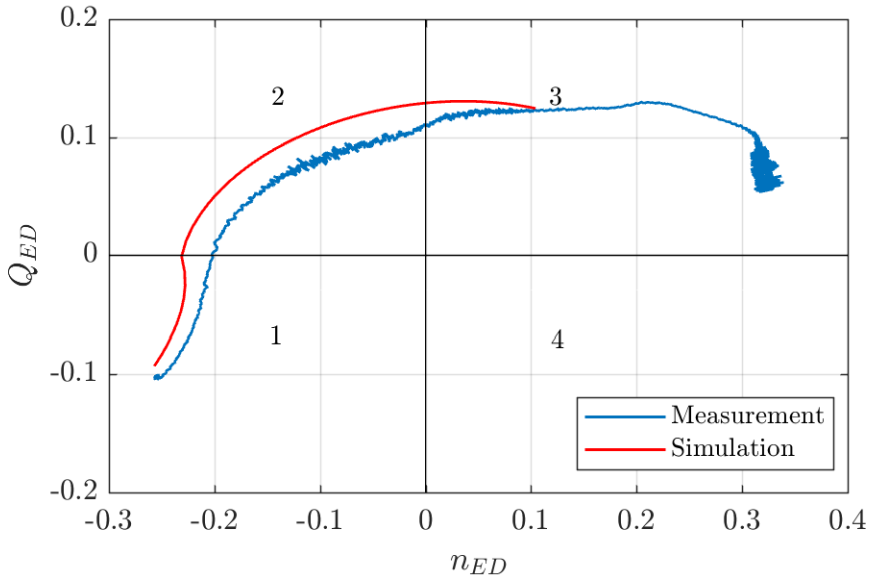

Figure 4.2: Transition from pump to turbine mode in n_{ED}-Q_{ED}-diagram

In the n_{ED}-Q_{ED}-diagram it is easier to see how the rotational speed changes during the transition from pump (1) to turbine mode (3). It shows how the simulation fails to reach the same rotational speed in turbine mode, as the simulation only reaches 1/3 of the value of n_{ED} from the measurements.

Non-dimensional time plots of the system variables during load rejection are presented in Figure 4.3 and 4.4, with the time span as the only difference.

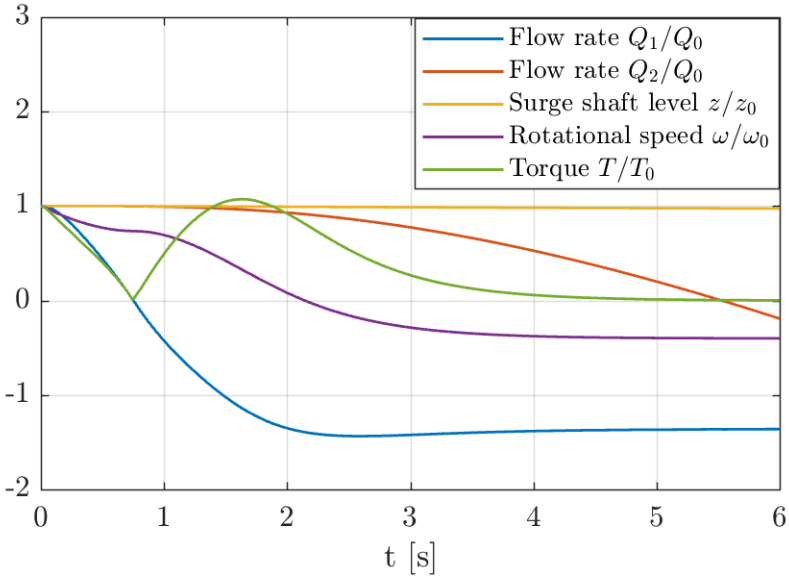

Figure 4.3: Results from simulation of load rejection, t_{max}= 6 s

After T_m is set to zero, the equilibrium between the motor torque and the hydraulic torque in Equation 2.35 is gone, and the hydraulic torque from the water drives the RPT from pump mode to turbine mode. The flow in the conduits start to decrease, and eventually turn to flow from the upper to the lower reservoir. When the flow through the runner (Q_1) becomes zero after about 0.75 s, the hydraulic torque does also go to zero, before it starts increasing when the flow becomes negative. The absolute value of the flow in the torque equation comes into play here, as the torque must be positive in order to drive the rotational speed to a higher negative value in turbine mode. After about 4 s the torque goes back to zero as the RPT reaches runaway speed, and the system converges towards a stationary solution.

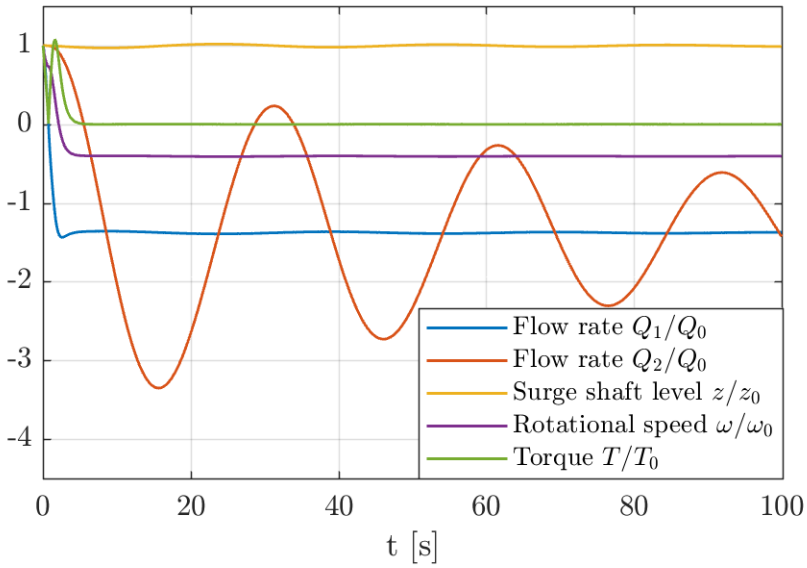

Figure 4.4: Results from simulation of load rejection, t_{max}= 100 s

Q_1 starts decreasing immediately after load rejection, while the decrease in Q_2 is delayed due to inertia in the system. Q_2 does experience large oscillations, which can be seen in Figure 4.4. The same oscillations can be found in the surge shaft level, but the amplitude is so small that it is hard to see them in the dimensionless plot.

The period of the oscillations is given by Equation 4.1 [13].

$$T = \frac{2\pi}{\sqrt{\frac{gA_T}{A_s L}}} \tag{4.1}$$

L is the length of the conduit between the surge shaft and the upper reservoir, A_s is the cross-sectional area of the surge shaft and A_T is the cross-sectional area of the conduit. $L = 13.9\ m$, $A_s = 3.8\ m^2$ and $A_T = 0.221\ m^2$ gives a period of 31.0 s, which is in good agreement with the period observed from Figure 4.4. This period is much greater than the time it takes for the hydraulic torque to get to zero, which means that the surge shaft level and the flow rate in the upper conduit continue to oscillate for a longer period of time before flow rate Q_2 converge towards the value of Q_1.

These oscillations do also cause small fluctuations in the hydraulic head and the rotational speed as all variables are causally interconnected in the system of ODEs, but the amplitudes of these oscillations are quite low. The oscillations in head can be seen in Figure 4.1 and 4.7 around the end points. Because the oscillations are relatively larger in head than in rotational speed, the head seems to fluctuate along a curve for constant rotational speed. The friction in the system has a large influence on the oscillations, which last longer in simulations than they would in reality because the friction factor is too low.

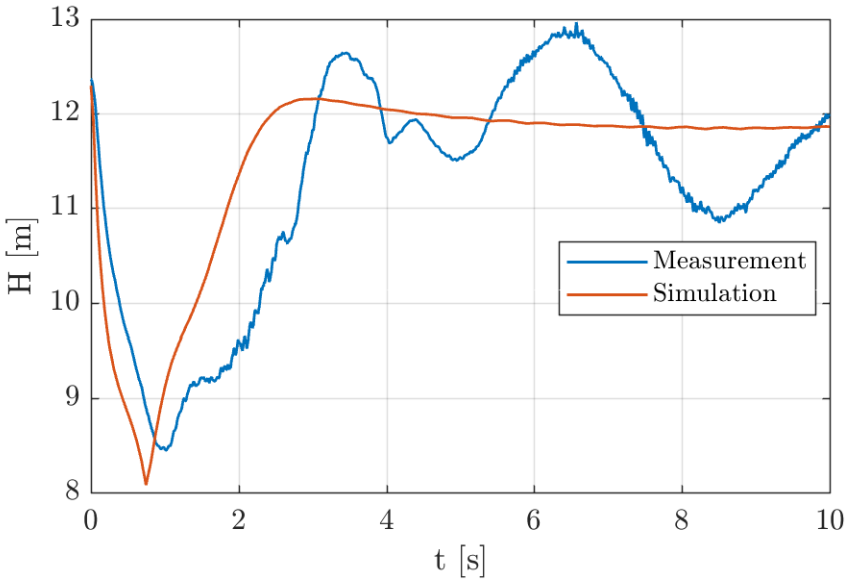

Figure 4.5: Comparison of the head during load rejection in measurement and simulation

The time plots of the head and rotational speed in Figure 4.5 and 4.6 show that the simulations roughly have the same time development as the measurements, although there are some deviations. I_h is inversely proportional to $\frac{\mathrm{d}Q}{\mathrm{d}t}$, while I_p is inversely proportional to $\frac{\mathrm{d}\omega}{\mathrm{d}t}$, according to the system of ODEs. This means that any deviation between the calculated and real value for these variables has a big influence on the transient development of the system. The time plot of the hydraulic head in Figure 4.5 suggests that I_h in the model might be too low because the flow reaches the minimum value at an earlier point than in the measurements. Regarding I_p it is harder to tell because of the large difference between the rotational speed in the measurements and in the simulations. This value is, however, calculated from time constant T_a that is measured in the laboratory, which means it should be fairly correct.

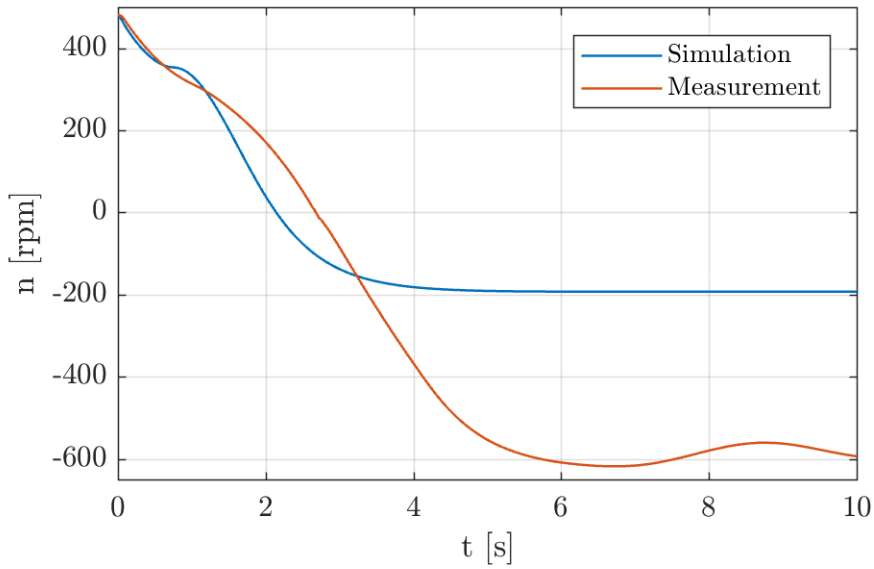

Figure 4.6: Comparison of the rotational speed during load rejection in measurement and simulation

4.2 Simulations of load rejection with modified pump-turbine characteristics

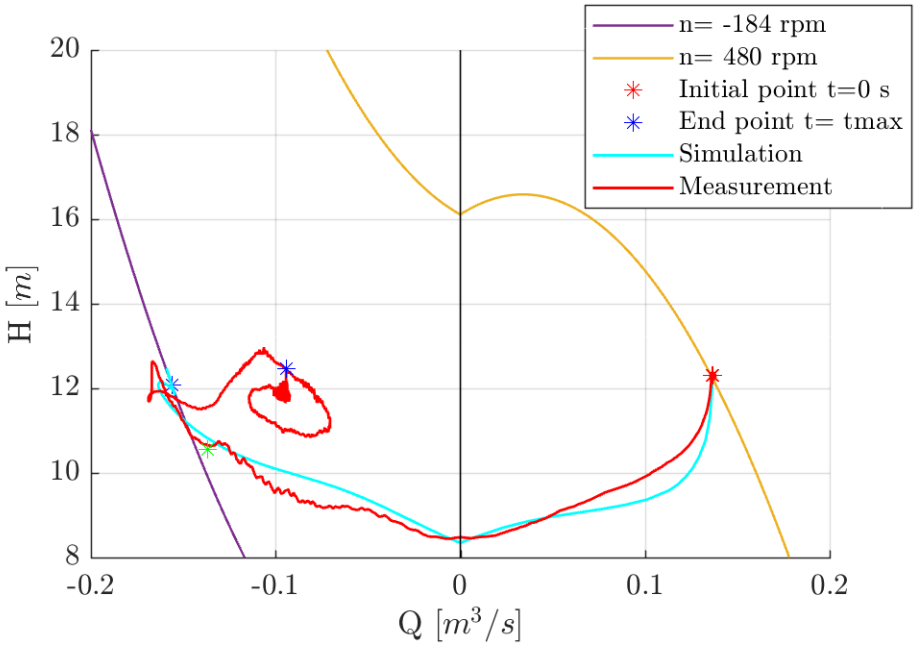

Figure 4.7: Transition from pump to turbine mode in H-Q-diagram, with modified characteristics

Figure 4.7 and 4.8 show the results when the characteristics are modified in order to make the measurement and simulation start at the same operating point. This is done by subtracting a head of 1.27 m in the model of the pump-turbine characteristics (Equation 2.31), a modification that changes the runaway speed to 184 rpm. Figure 4.7 reveals that the head in pump mode is generally higher in the measurement than in the simulation, while it is lower in pump brake mode. In n_{ED}-Q_{ED} the simulation and measurement match perfectly in pump mode, but they start to deviate right before the RPT enters pump brake mode. In this mode the difference increases slightly before the curves intersect in turbine mode right before the simulation ends with a much lower runaway speed than in the measurement.

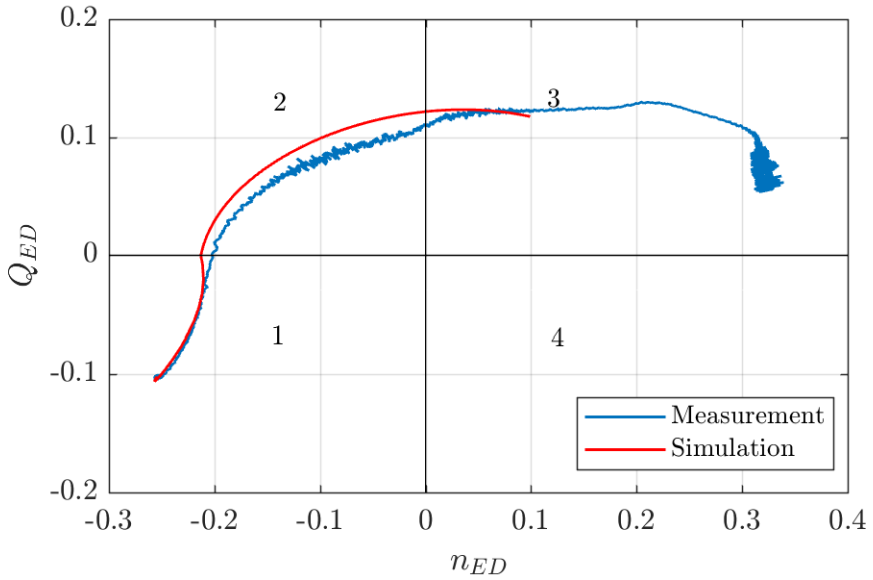

Figure 4.8: Transition from pump to turbine mode in n_{ED}-Q_{ED}-diagram, with modified characteristics

4.3 Characteristics based on measurements

Figure 4.9 shows a comparison between the model of the pump-turbine characteristics and derived characteristics. The latter are obtained using n_{ED} and Q_{ED}-values from measurements, and inserting constant rotational speeds of n=480 rpm and n=-480 rpm into Equation 3.1 and 3.2.

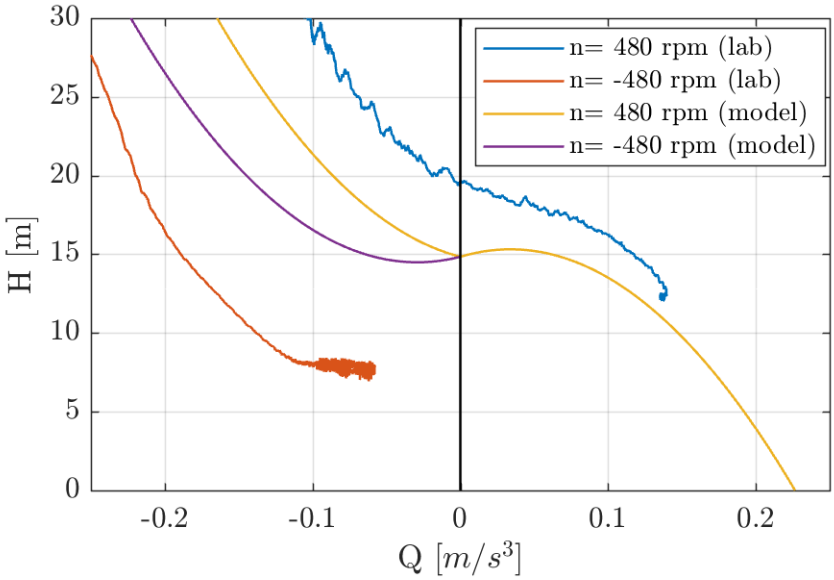

Figure 4.9: Pump-turbine characteristics based on measurements compared to model

By using Equation 3.3, the different parts of the characteristics in Figure 4.9 can be identified. Negative rotational speed produces the red graph in the second quadrant, which is turbine mode. Pump mode is the part of the blue graph located in the first quadrant, while pump brake is the part located in the second quadrant. Reverse pump mode would have taken place in the first quadrant at the continuation of the red curve, but the RPT does not enter into this mode of operation during load rejection.

5 | Discussion

Simulations and measurements from the laboratory show a fair agreement in pump mode and pump brake mode, but differ in turbine mode, as seen from Figure 4.1 and 4.2. The runaway speed is -194 rpm in the simulations, as opposed to -597 rpm in the measurements. The main reason for this is that the model of the pump-turbine characteristics is not sufficiently accurate in turbine mode, which will be discussed further.

Another difference between simulations and measurements can be seen in the H-Q-curves in Figure 4.1 and Figure 4.7, where the measured head fluctuates towards the end of the transition, while the simulated head does not. This is most likely a result of neglecting elasticity, rendering the model unable to simulate pressure pulsations that propagate through the conduits shortly after the transition. This can also be seen in Figure 4.5, where the fluctuations in the measured head are not present in the simulation.

The problem of causality in turbine mode does most likely also affect the dynamic behaviour of the system. In pump mode the torque from the motor sets the rotational speed, and the head depends on the rotational speed. In turbine mode, the chain of causation has switched, so that the head is now the controlling parameter. In the simulation program, however, the causality still works the same way it did in pump mode, namely by calculating the head for given flow and rotational speed. This could be a major reason why the simulations are not able to follow the same trajectory as the measurements in turbine mode, as seen in Figure 4.1 and 4.7.

In the non-dimensional plot of the system variables in Figure 4.3, the hydraulic torque goes to zero as the RPT passes through the point with zero flow after approximately 0.75 s. At this point, the simulation could be expected to stop because there is no hydraulic torque to drive the rotational speed to change. The rotational speed is almost constant around this point, but it starts decreasing again as the torque increases in turbine mode. The reason why this happens is probably the inertia in the system and the fact that the torque only approaches zero, and does not reach zero before it turns. When comparing the dynamic behaviour around 0.75 s to the stationary solution after 5 s, it becomes evident that the derivatives of all the variables go to zero around the latter point, while only the hydraulic

torque (the derivative of ω) goes to zero at the former point. Thus, the torque starts increasing again due to the change in flow. In reality, this problem is three-dimensional and there are flows present in different directions even when the one-dimensional flow is zero, which means that the hydraulic torque is not actually zero at this point. Comparisons between simulated and measured hydraulic torque have not been included in the results because no measurements of hydraulic torque were available.

The characteristics derived from the measurements, shown in Figure 4.9, reveal that the model predictions are not matching the measured characteristics. There is a deviation between the measurements and simulations in pump and pump brake, but it is worse in turbine mode. The difference in head between pump brake mode and turbine mode is also much higher in the measurements than in the model, and the head difference is proportional to the flow rate in the model, but not in the measurements. In Figure 4.9 the measured head in turbine mode and pump brake mode does not converge to the same point for zero flow, like they do in the model. Although there are no measurements around zero flow in turbine mode, there appears to be two different heads in the H-Q-characteristics for zero flow. The head is higher at the transition between pump and pump brake than between turbine and reverse pump mode. This is supported by Figure 5.1 [15]. The simulation model fails to take these differences into consideration, resulting in a too low runaway speed. The model curve for n=-480 rpm has a higher head than the measured curve, and a much lower rotational speed for a given static head at the runaway speed in turbine mode. Future models of the head in pump and turbine mode need to take this difference into account in order to obtain more accurate results.

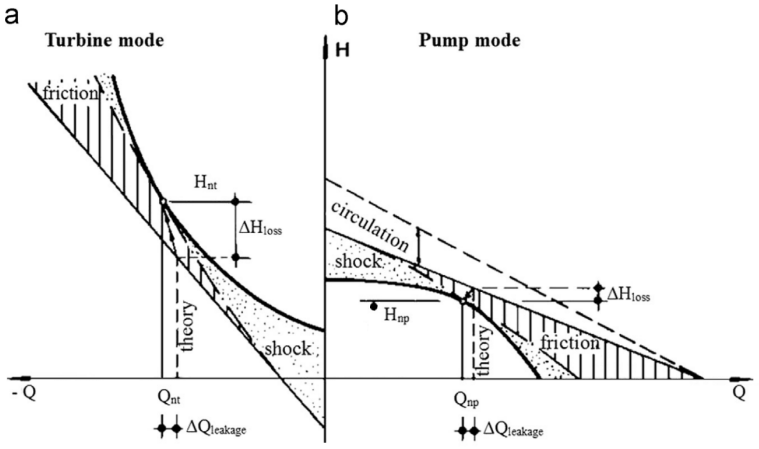

Figure 5.1: Pump and turbine characteristics [15]

Correction factors were implemented in order to see if this could make the simulation results more similar to the measurements. The head in turbine mode was divided by a factor that made the simulated head for n=-597 rpm equal to the measured head. A correction term, $R_m\omega^2$, representing the mechanical losses, which are disc friction losses and losses in bearings, was added to the torque equation, so that the hydraulic torque was equal to zero at n=-597 rpm. Intuitively one could expect that this would resolve the problems, and make the simulation match the measurements, but it turned out not to be the case. In the modified simulation, the head drops abruptly when the rotational speed switches, due to the large difference between the pump brake head and the turbine head for zero rotational speed, and the simulation converges to a stationary point of operation around -327 rpm and -0.23 m^3/s. The reason is because the torque goes to zero around this operating point as well as around -597 rpm, and as the simulation has to go through this point in order to get to -597 rpm, it stops there first. The results from this simulation are not reliable as the jump in head is nonphysical, and actually makes the characteristics deviate more from the measurement, instead of getting closer. In the original simulation model, there is no jump in head as the runner switches direction of rotation because the term that gives the head difference between pump brake mode and turbine mode, $a\frac{\omega}{\omega_0}Q$, is proportional to ω.

An interesting observation is that the head derived from the measurements is equal to zero for all flow rates when the rotational speed is zero, which can be seen by inserting $n = 0$ rpm into Equation 3.1 and 3.3. This means there is no jump in head when the rotational speed switches sign, and there are no friction losses to create a head loss over the RPT for nonzero flow rates in the derived characteristics, while there is such a head loss in the simulation model and in reality. Thus, there is a difference between the derived characteristics and reality, as well as between the simulation model and reality.

It is worth mentioning that stationary simulations starting at n=-597 rpm in turbine mode do not stay at this speed when the motor torque is disconnected, but slow down to -330 rpm. When the model is not able to operate at this point in stationary operation, it is not expected that it should do so in the transient simulations either.

The characteristics during dynamic operation are different from stationary operation due to the hydraulic inertia between the inlet and the outlet of the turbine [1]. In order to account for this, the head needs to be redefined according to Equation 5.1 in order to follow the stationary characteristics.

$$H_{dyn} = H - \frac{I_h}{g}\frac{\mathrm{d}Q}{\mathrm{d}t} \tag{5.1}$$

Future versions of the simulation model need to be modified in order to account for the hydraulic inertia of the water masses in the RPT when comparing the results to stationary characteristics. In this thesis, the simulations were compared to dynamic measurements, so this was not taken into account.

There are several other assumptions and simplifications in the model that need to be mentioned. One of them is the use of the Darcy-Weisbach equation for calculating the friction in the conduits of the RPT system. This equation is steady and one-dimensional, and does not yield accurate results for a problem that is transient and three-dimensional. It assumes a fully developed turbulent velocity profile, which is not a sound assumption for small flow rates or when the flow turns. Friction losses does also increase with the frequency, but this is not taken into account in this model. In general the model yields too low dampening, and especially for oscillations around zero flow [13]. A consequence of this is that the oscillations in Q_2 last more than 100 s, which is not very realistic. In order to compensate for the underestimated friction losses, the static head between the upper and lower reservoir in the simulations was set to 12.26 m instead of 11.8 m.

Figure 5.1 does also point out another difference between pump and turbine mode that the model does not take into account. In Equation 2.31 the losses in turbine mode are modelled by switching the signs from the losses in pump mode, but the figure shows that the impulse losses around zero flow are different in pump and turbine. The approach of using one model for the entire characteristics is based on the assumption that the velocity triangles are symmetrical in pump and turbine mode, which only holds true when slip, friction and impulse losses are neglected. Thus, the simulated characteristics differ from the measured ones.

In general, the implementation of losses in the system equations represent a source of error. Hydraulic losses are implemented in the hydraulic equation, but not in the torque equation. Mechanical losses are only implemented in the modified case, resulting in a runaway speed of -230 rpm for R_m=0.16 when the head is not corrected. A more accurate approximation of different losses would make the simulation results more equal to measurements.

A simplification that has not been subject to discussion up to this point is the replacement of the pressure chamber with a surge shaft in the simulation model. The pressure chamber is quite stiff, so a surge shaft with large area is a good replacement. However, the pressure chamber works more like an obstacle that is a source of friction, rather than a source of long period oscillations. Low frequency oscillations in Q_2 are present in the simulations, but not in the measurements, indicating that a better model of the pressure chamber could enhance the simulation results. However, the period of the oscillations is longer than the time it takes for the transition from pump to turbine mode, so this does not affect the the results of the transition to a high degree.

6 | Conclusion

The main objective of this thesis was to establish a simulation model of RPTs and use it to analyze the dynamic behaviour during the transition from pump to turbine mode. Simulations of transition from pump mode to turbine mode by cutting the torque were carried out, and a modified torque equation was successfully implemented to avoid breakdown as the rotational speed approached zero. Results from the simulations were in fair agreement with measurement data in pump and pump brake mode, but the runaway speed in turbine mode was too low compared with measurements.

It is more complicated than initially expected to represent both pump and turbine mode by the same model because there are two different heads in the pump-turbine characteristics for zero flow. They constitute two different modes of operation, and the model of the pump-turbine characteristics that was used in this thesis was based solely on pump mode, and it did not represent turbine mode with sufficient accuracy. Neglecting elasticity and the change of causality when the RPT goes from pump to turbine mode are other factors that influenced the simulation results and made the simulated head different from the measured head.

7 | Further work

The simulation model has been used to analyze a model scale RPT at the Waterpower Laboratory, and the next step would be to apply it to a full scale power plant like Tevla, which was originally planned, in order to see how the simulation would match the measurements. It would be interesting to see whether the model would perform differently on a full scale scale RPT compared to a laboratory scale, and to what degree the size of the runner, waterways etc comes into play regarding the model assumptions.

Before doing this, there are several modifications that should be done with the simulation model in order to improve the performance. The model of RPT characteristics need to be further developed in order to represent turbine mode more accurately. It must also be able to switch from pump brake mode to turbine mode without creating nonphysical jumps in the transient characteristics, as this happened in the simulations when implementing correction factors to account for the deviations. Based on the comparison between measurements and simulations, it seems like the approach of using one model of the characteristics to represent both pump and turbine mode might not necessarily be the best way to solve this problem. An approach that operates with one pump model and a different turbine model could be a solution if the transition is modelled appropriately. Other improvements would be to include elasticity and to model the losses more accurately. The differences in loss terms in pump and turbine mode needs to taken into account, and steady friction models like the Darcy-Weisbach equation are known for underestimating the dampening in transient phenomenon like load rejection, and could be improved. When simulating the RPT system at the Waterpower Laboratory, stationary measurements of the pump-characteristics were available for tuning the loss coefficients. This information is not available for a full size plant, making it more difficult to create an accurate simulation model of the pump-turbine characteristics.

Bibliography

[1] Nielsen, Torbjørn. *Transient characteristics of high head Francis turbines*. NTH, 1990.

[2] Tomescu, Mihai et al. *Renewable energy in Europe 2017*. European Environment Agency, 2017.

[3] Svarstad, Magni Fjørtoft. *Pumpe- og turbinkarakteristikker i fire kvadranter*. NTNU, 2014.

[4] Nielsen, Torbjørn. *Simulation model for Francis and Reversible Pump Turbines*. International Journal of Fluid Machinery and Systems (IJFMS), 2015.

[5] Walseth, Eve Cathrin. *Dynamic Behaviour of Reversible Pump-Turbines in Turbine Mode of Operation*. NTNU, 2016.

[6] Stranna, Andrea. *Testing of RPT in pumping mode of operation*. NTNU, 2013.

[7] Svarstad, Magni Fjørtoft. *Fast transition from pump to turbine mode of operation*. International Journal of Fluid Machinery and Systems (IJFMS), Aug. 2018 - accepted.

[8] Veie, Carl Andreas. *RPT in pump mode of operation*. NTNU, 2017.

[9] Nielsen, Torbjørn & Svarstad, Magni Fjørtoft. *Unstable behaviour of RPT when testing turbine characteristics in the laboratory*. IOP Conference Series: Earth and Environmental Science, 2014.

[10] Eve Cathrin Walseth. *Reversible Pump Turbines*. Youtube. 2010. URL: `https://www.youtube.com/watch?v=mpbWQbkl8_g#t=20m15s`.

[11] Brekke, Hermod. *Pumper og turbiner*. Water Power Laboratory, NTNU, 1999.

[12] Olimstad, Grunde. *Characteristics of Reversible-Pump Turbines*. NTNU, 2012.

[13] Nielsen, Torbjørn. *Dynamisk dimensjonering av vannkraftverk*. Water Power Laboratory, NTH, 1990.

[14] Brekke, Hermod. *Grunnkurs i hydrauliske strømningsmaskiner*. Water Power Laboratory, NTNU, 2000.

[15] Jain, Sanjay V. et al. *Investigations on pump running in turbine mode: A review of the state-of-the-art*. 2013.

Appendix A: Matlab code

```
clc
clear all
close all

% Constants
global a alpha2n A1 A2 As  beta1 beta2 B2 D1 D2 changeTm g H0 Hpt0 Hst
 Ih1 Ih2 Ip kf1 kf2 k1 k2 loadrejection L1 L2 omega0 omegaend omegamax
 Q0 Qstarmax rho z0
%geometrical constants of Olimstad rpt:
alpha2n=10*pi/180;
beta1=12.8*pi/180;
beta2=12*pi/180;
B2 = 0.0587;              % [m]
D1 = 0.349;               % [m] seen from pumpe mode
D2 = 0.6305;              % [m] seen from pump mode

%rpt system constants:
A1=0.17021; %area of pipe 1
A2=0.22187; %area of pipe 2
As=3.801254; %surge shaft area
g=9.821465; %gravity
Ih1=174.29;
Ih2=60.10;
Ip=17.76; %polar moment of intertia
kf1=2.043025; %friction loss pipe 1
kf2=0.42032; %friction loss pipe 2
L1=19.50; %length of pipe 1
L2=13.92; %length of pipe 2
omegamax=2*pi*560/60; %reference speed
rho=998.7; %water density
Qstarmax=0.1303; %design flow for reference speed

% Pump characteristics coefficients:
a=28.1261;
H0=24.165;
k1=179.5361;
k2=233.3412;

% Inputs
omega0=2*pi*input('Set the initial rotational speed (rpm): ')/60;
omegaend=2*pi*input('Set new rotational speed (rpm) to change the
 torque: ')/60; %changes the torque Tm=rho*g*Q*Hp/eta*omegaend after
 t=0 sec
changeTm=(omega0~=omegaend);
Hst=input('Set the static head (m) of the pump turbine system:
 '); %11.8 m VKL
tmax=input('Simulation time (s): ');
loadrejection=input('Load rejection/set Tm=0? (true/false): ');

% Error check
Qstar=Qstarmax*abs(omega0/omegamax);
if Hst>Hmax(omega0,Qstar) && omega0>0
```

```
    error('Error: The pump cannot deliever the required head (Hst) at
 this rotational speed. Increase n and/or decrease Hst.')
end

% Dynamic simulation
%y(1)=dQ1/dt
%y(2)=dQ2/dt
%y(3)=dz/dt
%y(4)=domega/dt

%Calculate Q0 at stationary operating point
Q0=operatingPoint(Hst,kf1,kf2,omega0); %calc. intersection between
 pump and system characteristics
Hpt0=getHpt(omega0,Q0);
z0=Hpt0-kf1*abs(Q0)*Q0; %using the first water way to find z0.
 Alternative: z0=Hst+kf2*|Q0|*Q0
y0=[Q0 Q0 z0 omega0]; %initial conditions
[t,Y]=ode45(@odefullsystem, [0,tmax], y0);
% Plot
figure(1)
plot(t,Y(:,1),t,Y(:,2),[0 tmax],[0 0],'k');
grid on
xlabel('Time t [s]')
ylabel('Volumetric flow rate Q [m^3/s]')
legend('Q1','Q2')

figure(2)
plot(t,Y(:,3));
grid on
xlabel('Time t [s]')
ylabel('Surge shaft level z [m]')

figure(3)
plot(t,60*Y(:,4)/(2*pi));
grid on
xlabel('Time t [s]')
ylabel('Rotational speed n [rpm]')

%Plot of pump characteristics
Qmin=-0.2; Qmax=0.2; Qstep=0.0001; rpmmin=2*pi*194/60;
 rpmmax=2*pi*480/60; rpmstep=rpmmax-rpmmin;
[Hptplot,Qplot,Htplot,Qtplot]=plotHpt(Qmin,Qmax,Qstep,rpmmin,...
    rpmmax,rpmstep);
rpm=[rpmmin,rpmmax];
for i=1:length(rpm)
    figure(4)
    hold all
    plot(Qplot,Hptplot(i,:),'lineWidth',0.9)
    plot(Qtplot,Htplot(i,:),'lineWidth',0.9)
    xlabel('Q [m^3/s]')
    ylabel('H [m]')
end

Hptend=getHpt(Y(length(Y),4),Y(length(Y),1));
```

```
figure(4)
grid on
plot(Q0,Hpt0,'r*',Y(length(Y),1),Hptend,'b*')%,[0 0],[0
 Hptplot(length(rpm),1)],'k',[Qmin Qmax],[0 0],'k')   %plot start
 point and end point of the transition
ylim([0 25])

%track the transition of operating point in HQ
Hpt_transition=transpose(getHptvec(Y(:,4),Y(:,1)));
if loadrejection || changeTm
    figure(4)
    plot(Y(:,1),Hpt_transition(:),'c');
end

figure(4)
legend('n= 194 rpm','n= -194 rpm','n= 480 rpm','n= -480 rpm','Initial
 point t= 0 s','End point t= tmax')

%spiral plot - convergence of surge shaft level vs flow
figure(5)
plot(Y(:,2),Y(:,3))
hold on
grid on
xlabel('Q [m^3/s]')
ylabel('Surge shaft level z [m]')

%time plot of the pump-turbine head
figure(6)
plot(t,Hpt_transition)
hold on
grid on
xlabel('Time t [s]')
ylabel('Pump-turbine head Hpt [m]')

%torque plot
Torque=getTorquevec(Y(:,4),Y(:,1));
figure(7)
plot(t,Torque)
hold on
grid on
xlabel('Time t [s]')
ylabel('Torque [Nm]')

%nondimensional plot
figure(8)
plot(t,Y(:,1)./y0(1),t,Y(:,2)./y0(1),t,Y(:,3)./y0(3),t,Y(:,4)./
y0(4),t,Torque./getTorque(y0(4),y0(1)));
grid on
legend('Q1','Q2','Surge shaft level z','Rotational speed n','Torque
 T')
```

Published with MATLAB® R2017a

```
function dy = odefullsystem(t,y)
global As changeTm g Hpt Hst Ih1 Ih2 Ip kf1 kf2 loadrejection omega0
 omegaend omegamax Q0 Qstarmax
%This function calculates the dervatives of the system variables y for
 each time step t

%dy(1)=dQ1/dt
%dy(2)=dQ2/dt
%dy(3)=dz/dt
%dy(4)=domega/dt
%dy(1)=g/Ih1*((Hpt-y(3))-kf1*abs(y(1))*y(1));
%dy(2)=g/Ih2*((y(3)-Hst)-kf2*abs(y(2))*y(2));
%dy(3)=(y(1)-y(2))/As;
%dy(4)=1/Ip*(Tm-Th);

dy=zeros(4,1);
Hpt=getHpt(y(4),y(1));
if t>0 && loadrejection
     Tm=0; %Tm=0 at load rejection
elseif t>0 && changeTm %for changing to a different rotational speed
     Qstar1=Qstarmax*abs(omegaend)/omegamax;
     Q1=operatingPoint(Hst,kf1,kf2,omegaend);
     Tm=getTorque(omegaend,Q1);
     if Hst>Hmax(omegaend,Qstar1) && omega0>0
         error('Error: The pump cannot deliever the required head
 (Hst) at this rotational speed. Modify n and/or Hst.')
     end
else %stationary operation
     Tm=getTorque(omega0,Q0);
end
dy(1)=g/Ih1*((Hpt-y(3))-kf1*abs(y(1))*y(1));
dy(2)=g/Ih2*((y(3)-Hst)-kf2*abs(y(2))*y(2));
dy(3)=(y(1)-y(2))/As;
dy(4)=1/Ip*(Tm-getTorque(y(4),y(1)));
end
```

Published with MATLAB® R2017a

```
%plots
load('C:\Users\carlav\Documents\Prosjektoppgave\New folder
\MagniMeasurement.mat');

Qed1=ndata(:,4);
ned1=ndata(:,5);

figure(20)
plot(ned1,Qed1,[0 0],[-0.2 0.2],'k',[-0.3 0.4],[0 0],'k')
grid on
xlabel('nED')
ylabel('QED')

Q480=ndata(:,8);
H480=ndata(:,9);
Q1=ndata(:,13);
H1=ndata(:,14);
Q2=smooth(Q1,500);
H2=smooth(H1,500);

Q560=ndata(:,27);
H560=ndata(:,28);
Q400=ndata(:,30);
H400=ndata(:,31);
Qny=ndata(:,34);
Hny=ndata(:,35);

n=-ndata(:,2);
Qplot1=-0.25:0.005:0.25;
omega=480;
a=28.1261;
H0=24.165;
k1=179.5361;
k2=233.3412;
Hp=(H0*omega^2/560^2-a*(omega)/560.*Qplot1-k1.*abs(Qplot1).*Qplot1-
k2*(0.1303*abs(omega)/560-abs(Qplot1)).*(0.1303*abs(omega)/560-
Qplot1));
omega=-480;
Qplot2=-0.25:0.005:0;
Ht=(H0*omega^2/560^2-a*(omega)/560.*Qplot2-k1.*abs(Qplot2).*Qplot2-
k2*(0.1303*abs(omega)/560-abs(Qplot2)).*(0.1303*abs(omega)/560-
Qplot2));
figure(21)
plot(Q480(1:164900),H480(1:164900),Q480(164901:length(Qny)),...
H480(164901:length(Hny)),Qplot1,Hp,Qplot2,Ht-8,[0 0],[0 30],...
'k','lineWidth',0.9)
legend('n= 480 rpm (measurement)','n= -480 rpm (measurement)', 'n= 480
 rpm (model)','n= -480 rpm (model)')
grid on
xlabel('Q [m^3/s]')
ylabel('H [m]')
```

```
figure(22)
plot(Q2,H2,'r',[0 0],[0
 20],'k',Q2(1),H2(1),'r*',Q2(length(Q2)),H2(length(H2)),'b*',...
-0.13684,10.55986,'g*')
grid on
xlabel('Q [m^3/s]')
ylabel('H [m]')

figure(4)
hold on
plot(Q2,H2,'r',Q2(1),H2(1),'r*',Q2(length(Q2)),H2(length(H2)),'b*',...
-0.13684,10.55986,'g*',[0 0],[0 25],'k',[-0.2 0.2],[0 0],'k')
legend('n= 180 rpm','n= -180 rpm','n= 480 rpm','n=
 -480 rpm','Initial point t=0 s','End point t=
 tmax','Simulation','Measurement')%,'Initial point t=0 sec','End point
 t=tmax','n=0 rpm')

fs=5000;
dt=1/fs;
tt=0:dt:(length(H1)/fs-dt);

figure(23)
plot(tt-30.33,H2)
hold on
plot(t,Hpt_transition)
legend('Measurement','Simulation')
grid on

%needs fullsystem to run
figure(24)
plot(Y(:,4),Torque)
grid on
xlabel('n [rpm]')
ylabel('T [Nm]')

%ted-ned
ned=(Y(:,4)./(2*pi)).*0.349./sqrt(9.81.*Hpt_transition);
Ted=Torque./(1000*9.81.*Hpt_transition.*0.349^3);
figure(25)
hold on
plot(-ned,Ted)
grid on
xlabel('nED [-]')
ylabel('TED [-]')

Qed=Y(:,1)./(0.349^2*sqrt(9.81.*Hpt_transition));
figure(26)
plot(ned1,Qed1,-ned,-Qed,'r',[0 0],[-0.2 0.2],'k',[-0.3 0.4],[0
 0],'k')
grid on
legend('Measurement','Simulation')
xlabel('nED')
ylabel('QED')
```

```
figure(27)
plot(t,60*Y(:,4)/(2*pi),'lineWidth',0.9)
hold on
plot(tt-30.33,n,'lineWidth',0.9)
grid on
legend('Simulation','Measurement')
```

Published with MATLAB® R2017a

```
function Hpt= getHpt(omega,Q)
%gives pump-turbine head for given omega and Q

global a H0 k1 k2 omegamax Qstarmax
Hpt=(H0*omega^2/omegamax^2-a*(omega)/omegamax*Q-k1*abs(Q)*Q-
k2*(Qstarmax*omega/omegamax-abs(Q))*(Qstarmax*omega/omegamax-Q));%
+1.2678;
end

function Hpt = getHptvec(omega,Q)
%gives pump-turbine head for a vector of given omega and Q

global a H0 k1 k2 omegamax Qstarmax
Hpt=zeros(1,length(omega));
for i=1:length(omega)
    Hpt(i)=(H0*omega(i)^2/omegamax^2-a*(omega(i))./
omegamax*Q(i)-k1*abs(Q(i))*Q(i)-k2*(Qstarmax*omega(i)/omegamax-
abs(Q(i)))*(Qstarmax*omega(i)./omegamax-Q(i)));%+1.2678;
end
end

function torque= getTorque(omega,Q)
%sets the hydraulic torque

global alpha2n beta1 beta2 B2 D1 D2 rho

%1=inlet pump 2=outlet pump
%input normal: y(4),y(1)
%input QO: omega0,Q0
%input Q1: omega1,Q1

A1=pi*D1^2/4;
A2=pi*D2*B2;
cm2=Q/A2;
u2=omega*D2/2;
cu2=u2-cm2/(tan(beta2));
alpha2=atan(cm2/cu2);
Rp=(D2/2)/(A2*tan(beta2))-(D1/2)/(A1*tan(beta1)); %shifting 1 and 2
torque=rho*abs(Q)*(D2/2*(Q/A2)*(cot(alpha2)+tan(alpha2n))-
D1^2/4*omega-Rp*Q+(D2^2-D1^2)/4*omega);%+0.168390*omega^2;
end
```

```
function torque= getTorquevec(omega,Q)
%sets the hydraulic torque for vector input

global alpha2n beta1 beta2 B2 D1 D2 rho

%1=inlet pump 2=outlet pump
%input normal: y(4),y(1)
%input QO: omega0,Q0
%input Q1: omega1,Q1

A1=pi*D1^2/4;
A2=pi*D2*B2;
cm2=Q./(A2);
u2=omega.*D2/2;
cu2=u2-cm2./(tan(beta2));
alpha2=atan(cm2./cu2);
Rp=(D2/2)/(A2*tan(beta2))-(D1/2)/(A1*tan(beta1)); %shifting 1 and 2
torque=rho.*abs(Q).*(D2/2.*(Q./A2).*(cot(alpha2)+tan(alpha2n))-
D1^2/4.*omega-Rp.*Q+(D2^2-D1^2)/4.*omega);%+0.168390.*omega.^2;
end

function f = operatingPoint(Hst,kf1,kf2,omega0)
tol=1;
Q=0;
while abs(tol)>10^(-3)
      Q=Q+0.000001*sign(omega0);
      Hp=getHpt(omega0,Q);
      Hs=Hst+(kf1+kf2)*abs(Q)*Q;
      tol=Hp-Hs;
end
f=Q;
end

function H= Hmax(omega,Qstar)
global a k1 k2 omegamax
%function that returns the highest possible head that a pump can
 deliver
%for one given rotational speed, found by differentiation
%Used for error check

Q=(2*k2*Qstar*omega/omegamax-a*omega/omegamax)/(2*(k1+k2));
H=getHpt(omega,Q);
end
```

```
function [Hptplot,Qplot,Htplot,Qtplot] =
 plotHpt(Qmin,Qmax,Qstep,rpmmin,rpmmax,rpmstep)
%For plotting the entire pump-turbine characteristics

global a H0 k1 k2 omega0 omegamax Qstarmax omegaend loadrejection

Qplot=Qmin:Qstep:Qmax;
Qtplot=Qmin:Qstep:0;
Htplot=zeros(1,length(Qtplot));
Hptplot=zeros(1,length(Qplot));

rpm=[rpmmin,rpmmax];
num=length(rpm);
for i=1:num
    rotspeed=(rpmmin-rpmstep)+i*rpmstep;
    Hptplot(i,:)=H0*(rotspeed/omegamax)^2-a*(rotspeed/
omegamax).*Qplot...
        -k1.*abs(Qplot).*Qplot-k2*(Qstarmax*rotspeed/omegamax-
abs(Qplot)).*(Qstarmax*rotspeed/omegamax-Qplot);%;+1.2678;
    if omega0<0 || omegaend<0 || loadrejection
        rotspeed1=(rpmmin-rpmstep)*sign(-1)+i*rpmstep*sign(-1);
        Htplot(i,:)=(H0*(rotspeed1/omegamax)^2-a*((rotspeed1)/
omegamax).*Qtplot...
        -k1.*abs(Qtplot).*Qtplot-k2*(Qstarmax*rotspeed1/omegamax-
abs(Qtplot)).*(Qstarmax*rotspeed1/omegamax-Qtplot));%+1.2678;%;
    end
end
end
```

Published with MATLAB® R2017a